Raul Guenther
Member, ABCM
guenther@emc.ufsc.br
Depto. Engenharia Mecânica
Universidade Federal de Santa Catarina-
88040-900 Florianópolis, SC, Brazil

Eduardo C. Perondi

perondi@emc.ufsc.br
Universidade Federal do Rio Grande do Sul
Rua Sarmento Leite 425
90050-170 Porto Alegre, RS, Brazil

Edson R. DePieri

edson@lcmi.ufsc.br
Depto. de Automação e Sistemas
Universidade Federal de Santa Catarina
88040-900 Florianópolis, SC, Brazil

Antônio C. Valdiero

valdiero@unijuí.tche.br
UNIJUÍ
98280-000 Panambi, RS, Brazil

Cascade Controlled Pneumatic Positioning System with LuGre Model Based Friction Compensation

This paper proposes a cascade controller with friction compensation based on the LuGre model. This control is applied to a pneumatic positioning system. The cascade methodology consists of dividing the pneumatic positioning system model into two subsystems: a mechanical subsystem and a pneumatic subsystem. This division allows the introduction of friction compensation at force level in the pneumatic positioning system. Using Lyapunov´s direct method, the convergence of the tracking errors is shown under the assumption that the system parameters are known. Experimental results illustrate the main characteristics of the proposed controller.
Keywords: *Servopneumatics, robotics, cascade control, friction compensation*

Introduction

Pneumatic positioning systems are very attractive for many applications because they are cheap, lightweight, clean, easy to assemble and present a good force/weight ratio. In spite of these advantages, pneumatic positioning systems possess some undesirable characteristics which limit their use in applications that require a fast and precise response. These undesirable characteristics derive from the high compressibility of the air and from the nonlinearities present in pneumatic systems.

To overcome the difficulties introduced by the high compressibility of the air and by the nonlinear air flow through the servovalve, a cascade control strategy has been developed in which the pneumatic positioning system is interpreted as an interconnected system: a mechanical subsystem driven by the force generated by a pneumatic subsystem (Guenther and Perondi, 2002).

Nonlinear friction is another important factor that affects the precision of the system position response. In pneumatic positioning systems the friction forces between the slider-piston system surfaces in contact are strongly dependent on the physical characteristics of the contacting surfaces, such as their material properties and geometry, and their lubrication conditions.

Classical friction models use static mappings that describe the steady state relation between velocity and friction force, which can be characterized by the viscous and Coulomb friction with Stribeck effect combination. However, some friction phenomena cannot be captured by static mapping, as for example, hysteretic behaviour with non-stationary velocity and breakaway force variations. Therefore, in the mechanics-related controller design, simple classical models are not sufficient to address applications with high-precision positioning requirements and low velocity tracking. Thus, to obtain accurate friction compensation and best control performance, friction forces model with dynamic behaviour is necessary (Armstrong et al., 1994).

A friction model that represents most of the steady state and dynamic friction properties, the LuGre model, has been proposed by Canudas de Wit et al. (1995). In this model, the friction force is modelled as the average deflection force of elastic bristles between two contacting surfaces. The tangential force applied to the contacting objects causes the bristles to deflect like springs. The average deflection is modelled by a first-order nonlinear differential equation, which describes the dynamic behaviour of the overall friction force.

Although friction compensation is especially important for pneumatic devices, it is particularly difficult to be performed using non-model based compensation or even model-based compensation (see Armstrong et al., 1994). The model-based friction compensation, adopted in this work, uses an on-line friction force estimation scheme. The compensation is achieved by adding the estimated friction force to the reference force generated by the position controller at the force level. To use this compensation scheme it is usually assumed that the actuator has a fast and accurate force response (Canudas de Wit et al., 1995, Lischinsky et al., 1999). This assumption is generally verified for positioning systems with electric actuators and sometimes for positioning systems with hydraulic actuators. Nevertheless, most pneumatic positioning systems do not provide a sufficiently fast and efficient force response.

The cascade control strategy adopted in this work allows us to introduce the friction compensation at the force level without any assumption about the actuator force response. This occurs because, according to this strategy, the mechanical subsystem is driven by the force generated in the pneumatic subsystem. So, it is possible to introduce the friction compensation by adding the estimated friction force at the mechanical subsystem, *i.e.*, at the force level. It should be remarked that the friction force observer proposed by Canudas de

Wit et al. (1995) requires slight modifications to be applied in the cascade control scheme.

This paper presents a cascade controller scheme that applies the LuGre model friction compensation technique to a pneumatic positioning system. The convergence of the tracking errors is demonstrated using the Lyapunov direct method when all the system parameters are known and there are no external forces. Experimental results illustrate the main properties of the proposed controller.

This paper is organized as follows. In Section 2, the experimental test rig is described. Section 3 is dedicated to the presentation of the theoretical model of the investigated system, while, in Section 4, the cascade controller and the proposed friction force estimator are described. The controller stability properties are stated in Section 5. In Section 6, the experimental results are presented. Finally, the main conclusions are outlined in Section 7.

Nomenclature

A = piston area, m^2
c_p = air specific heat at constant pressure, J/Kg K
c_v = air specific heat at constant volume, J/Kg K
$d(t)$ = disturbance
$\boldsymbol{D}$ = tracking error matrix
$e(t)$ = error function
F = force, N
F_a = friction force, N
F_c = Coulomb friction force, N
F_e = external forces, N
F_s = static friction force, N
$\boldsymbol{g}$ = continuous vector force, N
$g(t)$ = action force, N
$g_d(t)$ = desired action force, N
$H(s)$ = generic transfer function
$\hat{h}$ = pneumatic subsystem dynamics independent of the control voltage
$\boldsymbol{I}$ = identity matrix
K = positive gain
K_D = cascade controller's positive gain
K_o = positive gain
K_P = cascade controller's positive pressure gain
k_v = real positive constant
L = piston stroke, m
M = mass, Kg
$m(.)$ = smoothing function
$\boldsymbol{N}$ = state dependent matrix
p = absolute pressure, Pa
p_Δ = pressure drop, Pa
P = real positive constant
$P_{\Delta\delta}$ = desired pressure drop, Pa
Q = heat transfer energy, J
q_m = mass flow rate, Kg/s
Q_N = nominal volumetric flow rate $[m^3/s]$
R = gas constant, KgJ/K
$\boldsymbol{R}$ = residual set
r = specific heat ratio, dimensionless
s = velocity error function, m/s
s = Laplace operator
T = temperature, K
t = time, s
u = control voltage signal, V
u_a = auxiliary signal
u_a^* = ideal auxiliary signal
$\hat{u}$ = pneumatic subsystem dynamics dependent of the control voltage, m^3/s

V_{10} = fixed volume at chamber 1 end of the stroke, m^3
V_{20} = fixed volume at chamber 2 end of the stroke, m^3
V = non negative scalar function, Lyapunov´s function
$y(t)$ = piston position, m
$y_d(t)$ = desired piston position, m
$y_{máx}$ = extreme desired position, m
$\dot{y}_r$ = reference velocity, m/s
$\dot{y}_s$ = threshold Stribeck velocity, m/s
z = presliding displacement

Greek Symbols

γ = maximum/minimum eigenvalue ratio, bounded real number
η = constant that measures trajectory speed
λ = cascade controller's gain
λ_{max} = maximum eigenvalue
λ_{min} = minimum eigenvalue
ρ = density [Kg/m^3]
$\boldsymbol{\rho}$ = closed loop tracking error
σ_0 = elastic stiffness coefficient [N/m^2]
σ_{0e} = estimated elastic stiffness coefficient [N/m^2]
σ_1 = friction coefficient [Ns/m]
σ_2 = viscous friction coefficient [Ns/m]
ω = frequency [rad/s]
Ω = a specific domain
ϖ_n = natural frequency [rad/s]
ζ = dumping ratio, dimensionless

Subscripts

$*$ relative to exact or known value
0 relative to initial or normalized conditions
1 relative to cylinder's chamber 1
2 relative to cylinder's chamber 2
d relative to desired condition
I relative to initial condition
max relative to maximum value condition
min relative to minimum value condition
N relative to nominal value
r relative to reference signal
Δ relative to gradient

The Pneumatic Positioning System

The system under consideration is shown in Fig.1. It consists of a proportional servovalve 5/3 (MPYE-5-1/8 FESTO) that drives a double action rodless cylinder, with internal diameter of 0.025 [m] and 1 [m] stroke (DGPL-1000 FESTO).

The measured nominal flow rate is $Q_N = 7.10^3$ [m^3/s] (420 [L/min]) and, due to an internal feedback, it is independent of the supply pressure. This fact assures an approximately linear behaviour of the valve opening. A small overlap causes a 4% dead-zone. The piston is connected to a linear sensor (Festo POT-1000-TFL), with a stroke equal to the cylinder stroke (1.0 [m]). The absolute pressure in each cylinder chamber and the supply pressure are measured through three piezoelectric pressure sensors. The control and data acquisition apparatus consists of a control board (dSPACE GmbH – DS1102) and an IBMPC Pentium 100MHz microcomputer. The sampling time is 1 [ms].
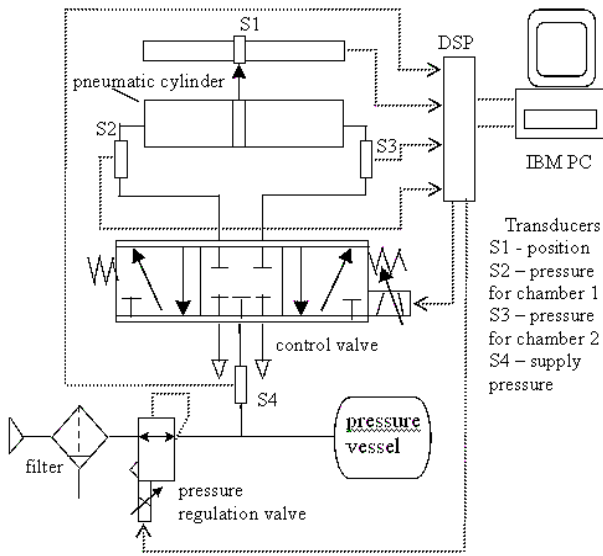
Figure 1. Experimental rig.

The Dynamic Model

The dynamic model used in this work is developed based on: **(i)** the description of the relationship between the air mass flow rate and pressure changes in the cylinder chambers, and **(ii)** the equilibrium of the forces acting at the piston, including the friction force.

The relationship between the air mass flow rate and the pressure changes in the chambers is obtained using energy conservation laws, and the force equilibrium is given by Newton's second law. The friction force is included in the LuGre friction model.

Conservation of Energy

The internal energy of the mass flowing into chamber 1 is $C_p q_{m1} T$, where C_p is the constant pressure specific heat of the air, T is the air supply temperature, and $q_{m1} = (dm_1/dt)$ is the air mass flow rate into chamber 1. The rate at which work is done by the moving piston is $p_1 \dot{V}_1$, where p_1 is the absolute pressure in chamber 1 and $\dot{V}_1 = (dV_1/dt)$ is the volumetric flow rate. The time air internal energy change rate in the cylinder is $d(C_V \rho_1 V_1 T)/dt$, where C_V is the constant volume specific heat of the air and ρ_l is the air density. We consider the ratio between the specific heat values as $r = C_P/C_V$ and that $\rho_1 = C_V/(RT)$ for an ideal gas, where R is the universal gas constant. An energy balance yields

$$q_{m1}T - \frac{p_1}{C_P}\frac{dV_1}{dt} = \frac{1}{rR}\frac{d}{dt}(p_1 V_1) \qquad (1)$$

where the rate of heat transfer through the cylinder walls ($\dot{Q}$) is considered negligible. The total volume of chamber 1 is given by $V_1 = Ay + V_{10}$, where A is the cylinder cross-sectional area, y is the piston position and V_{10} is the dead volume of air in the line and at the chamber 1 extremity. The change rate for this volume is $\dot{V}_1 = A\dot{y}$, where $\dot{y} = dy/dt$ is the piston velocity. After calculating the derivative term in the right hand side of (1) we can solve this equation to obtain

$$\dot{p}_1 = -\frac{Ar\dot{y}}{Ay+V_{10}}p_1 + \frac{RrT}{Ay+V_{10}}q_{m1} \qquad (2)$$

where $C_p = (rR)/(r-1)$.

Similarly for chamber 2 of the cylinder we obtain

$$\dot{p}_2 = \frac{Ar\dot{y}}{A(L-y)+V_{20}}p_2 + \frac{RrT}{A(L-y)+V_{20}}q_{m2} \qquad (3)$$

where L is the cylinder stroke.

Assuming that the mass flow rates are nonlinear functions of the servovalve control voltage (u) and of the cylinder pressures, that is, $q_{m1} = q_{m1}(p_1,u)$ and $q_{m2} = q_{m2}(p_2,u)$, expressions (2) and (3) result in

$$\dot{p}_1 = -\frac{Ar\dot{y}}{Ay+V_{10}}p_1 + \frac{RrT}{Ay+V_{10}}q_{m1}(p_1,u) \qquad (4)$$

$$\dot{p}_2 = \frac{Ar\dot{y}}{A(L-y)+V_{20}}p_2 + \frac{RrT}{A(L-y)+V_{20}}q_{m2}(p_2,u) \qquad (5)$$

Piston Dynamics

Applying Newton's second law to the piston-load assembly results in

$$M\ddot{y} + F_a + F_e = A(p_1 - p_2) \qquad (6)$$

where M is the mass of the piston-load assembly, F_a is the friction force, F_e is the external force and $A(p_1 - p_2)$ is the force related to the pressure difference between the two sides of the piston (see Fig. 2).
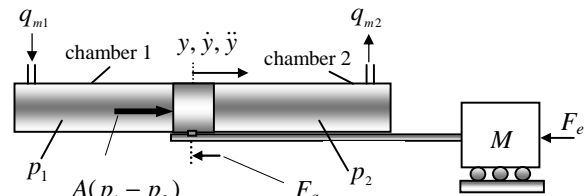

Figure 2. Force equilibrium at the piston.

Friction Model

In this paper the friction force (F_a) is described according to the LuGre friction model proposed by Canudas et al. in [2]. This model satisfies the requirements for friction compensation in pneumatic systems because it can describe complex friction behavior, such as stick-slip motion, presliding displacement, Dahl and Stribeck effects and frictional lag.

In this model the friction force is given by

$$F_a = \sigma_0 z + \sigma_1 \frac{dz}{dt} + \sigma_2 \dot{y} \qquad (7)$$

where z is a friction internal state that describes the average elastic deflection of the contact surfaces during the stiction phases, the parameter σ_0 is the stiffness coefficient of the microscopic

deformations z during the presliding displacement, σ_1 is a damping coefficient associated with dz/dt and σ_2 represents the viscous friction. The dynamics of the internal state z are expressed by

$$\frac{dz}{dt} = \dot{y} - \frac{|\dot{y}|\sigma_0}{g(\dot{y})}z \qquad (8)$$

where $g(\dot{y})$ is a positive function that describes the "steady-state" characteristics of the model for constant velocity motions and is given by

$$g(\dot{y}) = F_c + (F_s - F_c)e^{-(\dot{y}/\dot{y}_s)^2} \qquad (9)$$

where F_c is the Coulomb friction force, F_s is the static friction force and $\dot{y}_s$ is the Stribeck velocity. In equation (9) it can be observed that $g(\dot{y})$ is bounded by the static friction force F_s.

An important property of the LuGre friction model is that the average elastic deflection z is bounded. This statement can be outlined by considering the following Lyapunov candidate function:

$$V = \tfrac{1}{2}z^2 \qquad (10)$$

Differentiating (10) and combining with equation (8), it can be written:

$$\frac{dV}{dt} = -|\dot{y}| \cdot |z| \cdot \left(\frac{\sigma_0 \cdot |z|}{g(\dot{y})} - sign(\dot{y}) \cdot sign(z)\right) \qquad (11)$$

The time derivative of the Lyapunov candidate function dV/dt given in (11) is negative if $|z > g(\dot{y})/\sigma_0$, since $g(\dot{y})$ is strictly positive and bounded by F_s (see equation (9)). It results that the set $\Pi = \{z: |z| \leq F_s/\sigma_0\}$ is an invariant set for the solutions of equation (8), and that the elastic deflection z is bounded.

The Interconnected Model

Equations (4), (5), (6), (7) and (8) constitute a fifth order nonlinear dynamic model of the pneumatic positioning system with friction. To rewrite this model in an interconnected form, appropriate for our cascade controller design, we define

$$M\ddot{y} + F_a + F_e = Ap_\Delta \qquad (12)$$

The pressure difference change rate, calculated using expressions (4) and (5), is given by

$$\dot{p}_\Delta = RrT\left[\frac{q_{m1}(p_1,u)}{Ay+V_{10}} - \frac{q_{m2}(p_2,u)}{A(L-y)+V_{20}}\right]$$
$$- rA\dot{y}\left[\frac{p_1}{Ay+V_{10}} + \frac{p_2}{A(L-y)+V_{20}}\right] \qquad (13)$$

Separating $\dot{p}_\Delta$ into the terms affected by the servovalve control voltage u and the terms which are functions only of piston position and velocity, we obtain the functions $\hat{u} = \hat{u}(p_1,p_2,y,u)$ and $\hat{h} = \hat{h}(p_1,p_2,y,\dot{y})$, given, respectively, by

$$\hat{u}(p_1,p_2,y,u) = RrT\left[\frac{q_{m1}(p_1,u)}{Ay+V_{10}} - \frac{q_{m2}(p_2,u)}{A(L-y)+V_{20}}\right] \qquad (14)$$

$$\hat{h}(p_1,p_2,y,\dot{y}) = -rA\dot{y}\left[\frac{p_1}{Ay+V_{10}} + \frac{p_2}{A(L-y)+V_{20}}\right] \qquad (15)$$

This allows us to rewrite expression (13) as

$$\dot{p}_\Delta = \hat{h}(p_1,p_2,y,\dot{y}) + \hat{u}(p_1,p_2,y,u) \qquad (16)$$

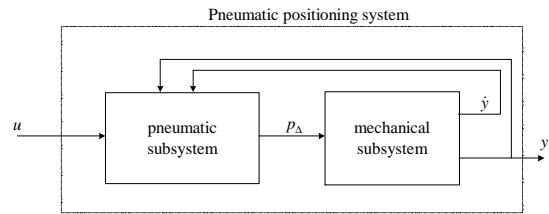Equations (12) and (16) describe the pneumatic positioning system dynamics.

Figure 3. Pneumatic system described as two interconnected subsystems.

Equation (12) represents the mechanical subsystem driven by a pneumatic force $g = Ap_\Delta$. Equation (16) describes the dynamics of the pneumatic subsystem in which this pneumatic force is generated by commanding the control voltage u appropriately. This interpretation reinforces the interconnected model description (Fig.3).

The Cascade Control Strategy

We present here the cascade control strategy based on the methodology of order reduction described in Utkin (1987). This cascade control strategy has been used successfully in the control of robot manipulators with electric actuators (Guenther and Hsu, 1993), to control flexible joint manipulators (Hsu and Guenther, 1993) and hydraulic actuators (Guenther and De Pieri, 1997, Cunha et al., 2002).

According to this strategy, the pneumatic positioning system is interpreted as an interconnected system like that presented in Fig.3 and its equations can thus be rewritten in a convenient form. To perform this task we initially define the pressure difference tracking error as

$$\tilde{p}_\Delta = p_\Delta - p_{\Delta d} \qquad (17)$$

where $p_{\Delta d}$ is the desired pressure difference to be defined based on the desired force $g_d = Ap_{\Delta d}$. This is the desired force required on the piston-load assembly mass to obtain a desired tracking performance. Using the definition (17), equations (12) and (16) may be rewritten as

$$M\ddot{y} = Ap_{\Delta d} + d(t) \qquad (18)$$

$$\dot{p}_\Delta = \hat{h}(p_1,p_2,y,\dot{y}) + \hat{u}(p_1,p_2,y,u) \qquad (19)$$

where $d(t)$ is an input disturbance given by

$$d(t) = A\tilde{p}_\Delta - F_a - F_e \qquad (20)$$

The system (18)(19) is in the cascade form. Equation (18) can be interpreted as a mechanical subsystem driven by a desired force $g_d = Ap_{\Delta d}$ and subjected to an input disturbance $d(t)$. Equation (19) represents the pneumatic subsystem.

The design of the cascade controller for the system (18)(19) can be summarized as follows:

(i) – Compute a control law $g_d(t) = Ap_{\Delta d}(t)$ for the mechanical subsystem (18) such that the piston displacement ($y(t)$) achieves a desired trajectory $y_d(t)$ taking into account the presence of the disturbance $d(t)$; and then

(ii) – Compute a control law $u(t)$ such that the pneumatic subsystem (19) applies a pneumatic force $g(t) = Ap_\Delta(t)$ to the mechanical subsystem that tracks the desired force $g_d(t) = Ap_{\Delta d}(t)$.

In this paper the design of the mechanical subsystem control law $g_d(t)$ is based on the controller proposed by Slotine and Li (1988), including a friction compensation scheme based on the LuGre friction model. The control law $u(t)$ is synthesized to achieve good tracking performance characteristics related to the pneumatic subsystem.

Friction Force Observer

According to Canudas de Wit et al. (1995) the estimated friction force $\hat{F}_a$ is given by

$$\hat{F}_a = \sigma_0 \hat{z} + \sigma_1 \frac{d\hat{z}}{dt} + \sigma_2 \dot{y} \qquad (21)$$

where $\hat{z}(t)$ is the estimated friction internal state given by

$$\frac{d\hat{z}}{dt} = \dot{y} - \frac{|\dot{y}|\sigma_0}{g(\dot{y})}\hat{z} - K_0\tilde{y} \qquad (22)$$

and K_0 is a positive constant.

In Canudas de Wit et al. (1995) the authors show that the friction force observer (21)(22) applied to an electric actuator leads the position error $\tilde{y}(t)$ to converge asymptotically to zero if the electric actuator position controller is designed such that the dynamic relating the position error $\tilde{y}(t)$ and the estimation error $\tilde{z}(t) = z(t) - \hat{z}(t)$ is strictly positive real (SPR).

The observer (22) requires a slight modification to be used within the cascade control scheme. This modification is required because the value of the friction force time change rate $\dot{F}_a$ is used to calculate the control signal in the cascade control strategy. So, the function $|\dot{y}|$ has to be smoothed by a function $m(\dot{y})$ (like $m(\dot{y}) = (2/\pi)\dot{y}\arctan(k_v\dot{y})$, where k_v is a positive constant, for example). Note that, as with the function $|\dot{y}|$, the function $m(\dot{y})$ is equal to zero at the origin ($m(0) = 0$).

Additionally, to achieve the desired stability properties for the pneumatic positioning system closed loop, it is proposed in this paper that the internal state $\hat{z}(t)$ is estimated using the following modified observer

$$\frac{d\hat{z}}{dt} = \dot{y} - \frac{m(\dot{y})\sigma_0}{g(\dot{y})}\hat{z} - \sigma_0 Ks \qquad (23)$$

where K is a positive constant and s is the measure of the velocity tracking error defined in equation (27).

Introducing the function $m(\dot{y})$, the residual difference $\Delta(\dot{y}) \geq 0$ is defined as

$$\Delta(\dot{y}) = |\dot{y}| - m(\dot{y}) \qquad (24)$$

and the friction internal state estimating error $\tilde{z}(t)$ is given by

$$\frac{d\tilde{z}}{dt} = -\frac{m(\dot{y})\sigma_0}{g(\dot{y})}\tilde{z} - \frac{\Delta(\dot{y})\sigma_0}{g(\dot{y})}z + \sigma_0 Ks \qquad (25)$$

Tracking Control of the Mechanical Subsystem

Based on Slotine and Li (1988) and including the friction compensation, the following control law to obtain trajectory tracking in the mechanical subsystem is proposed:

$$g_d = M\ddot{y}_r - K_D s + \hat{F}_a \qquad (26)$$

where K_D is a positive constant, $\dot{y}_r$ is the reference velocity and s is a measure of the velocity tracking error.

In fact, $\dot{y}_r$ can be obtained by modifying the desired velocity $\dot{y}_d$ as follows

$$\dot{y}_r = \dot{y}_d - \lambda\tilde{y} \; ; \; \tilde{y} = y - y_d ; \qquad s = \dot{y} - \dot{y}_r = \dot{\tilde{y}} + \lambda\tilde{y} \qquad (27)$$

where λ is a positive constant.

Let the friction force be given according to the LuGre friction model (7). Substituting (26) in (18) and using definition (20) and the observer (21)(23), the error equation related to the mechanical subsystem becomes

$$M\dot{s} + K_D s + \sigma_1\dot{\tilde{z}} + \sigma_0\tilde{z} = A\tilde{p}_\Delta - F_e \qquad (28)$$

Consider the non-negative function

$$2V_1 = Ms^2 + K^{-1}\tilde{z}^2 \qquad (29)$$

Using (25) and (28), the time derivative of (29) along the mechanical subsystem trajectories is given by

$$\dot{V}_1 = -(K_D + \sigma_1\sigma_0 K)s^2 + A\tilde{p}_\Delta s - \frac{m(\dot{y})\sigma_0 K^{-1}}{g(\dot{y})}\tilde{z}^2 + \frac{m(\dot{y})\sigma_0\sigma_1}{g(\dot{y})}s\tilde{z}$$
$$+ \frac{\sigma_0\sigma_1\Delta(\dot{y})}{g(\dot{y})}zs - F_e s - K^{-1}\frac{\sigma_0\Delta(\dot{y})}{g(\dot{y})}z\tilde{z} \qquad (30)$$

Expression (30) will be used in the stability analysis.

Tracking Control of the Pneumatic Subsystem

In order to obtain force tracking in the pneumatic subsystem (19) we propose the following control law

$$\hat{u} = u_a - K_P\tilde{p}_\Delta - As \qquad (31)$$

where u_a is an auxiliary control signal, K_P is a positive constant, A is the cylinder cross-sectional area, and s is defined in (27).

Substituting (31) in (19), the resulting pneumatic subsystem closed loop dynamics gives

$$\dot{p}_\Delta = \hat{h}(p_1, p_2, y, \dot{y}) + u_a - K_p \tilde{p}_\Delta - As \qquad (32)$$

The designs of the auxiliary signal u_a and of the constant K_P are based on the non-negative function V_2 defined as

$$2V_2 = \tilde{p}_\Delta^2 \qquad (33)$$

The time derivative of (33) is given by $\dot{V}_2 = \tilde{p}_\Delta (\dot{p}_\Delta - \dot{p}_{\Delta d})$, where the time derivative of the desired pressure difference ($\dot{p}_{\Delta d} = \dot{g}_d / A$) is obtained using (26). So, in order to calculate $\dot{p}_{\Delta d}$, we need to know the acceleration signal. In the ideal case (where all the parameters are known and there is no friction or external forces), the acceleration may be calculated using expression (6) by means of the pressure difference p_Δ measurement.

The time derivative of (33) along the pneumatic subsystem trajectories is obtained using the closed loop dynamics (32):

$$\dot{V}_2 = \tilde{p}_\Delta [u_a + \hat{h} - \dot{p}_{\Delta d} - K_P \tilde{p}_\Delta - As] \qquad (34)$$

Defining the ideal auxiliary signal as

$$u_a^* = \dot{p}_{\Delta d} - \hat{h}(p_1, p_2, y, \dot{y}) \qquad (35)$$

results in

$$\dot{V}_2 = \tilde{p}_\Delta [\Delta u_a - K_P \tilde{p}_\Delta - As] \qquad (36)$$

where $\Delta u_a = u_a - u_a^*$ is the auxiliary signal error. In the ideal case, $u_a = u_a^*$, $\Delta u_a = 0$, and expression (36) results in

$$\dot{V}_2 = -K_P \tilde{p}_\Delta^2 - As\tilde{p}_\Delta \qquad (37)$$

Expression (37) will also be used in the stability analysis.

The Pneumatic Positioning System Controller

The pneumatic positioning system cascade controller is a combination of the mechanical subsystem position tracking control law (26) and the control signal designed to obtain the pneumatic subsystem tracking force (31).

Using (26) we calculate the desired pressure difference to obtain the trajectory tracking in the mechanical subsystem, $p_{\Delta d} = g_d / A$.

In the ideal case, in which $u_a = u_a^*$, the signal $\hat{u}$ is calculated using equations (31) and (35). The necessary time derivative of the desired pressure difference is obtained as described above, and the function $\hat{h} = \hat{h}(p_1, p_2, y, \dot{y})$ as defined in (15).

The servovalve control voltage u is obtained through the inverse of the function (14), that is,

$$u = u(p_1, p_2, y, \hat{u}) \qquad (38)$$

The use of the inverse defined in (38) and the function $\hat{h} = \hat{h}(p_1, p_2, y, \dot{y})$ in the control law may be interpreted as a feedback linearization scheme (see Khalil, 1996).

Stability Analysis

Consider the cascade controlled pneumatic positioning system with the friction observer. In this case the closed loop system is $\Omega = \{(12),(16),(21),(23),(26),(31)\}$.

We assume that the desired piston position $y_d(t)$ and its derivatives, up to 3rd order are uniformly bounded.

For the ideal case, in which all the system parameters are known and there is no external force F_e, the tracking errors convergence properties are stated below.

Theorem – When all the system parameters are known and there is no external force F_e, given an initial condition, the controller gains can be chosen in order to obtain the convergence of the tracking errors, $\dot{\tilde{y}}(t)$ and $\tilde{y}(t)$, to a residual set R as $t \to \infty$. The set R depends on the friction characteristics and the controller gains.

Proof: Consider the lower bounded function

$$2V(t) = 2V_1 + 2V_2 = Ms^2 + \tilde{p}_\Delta^2 + K^{-1}\tilde{z}^2 \qquad (39)$$

where the functions V_1 and V_2 are defined in (29) and (33), respectively.

This expression can be written in the following matrix equation form

$$V = \frac{1}{2}\rho^T N_1 \rho \qquad (40)$$

where the error state vector is defined as $\rho = [s \quad \tilde{p}_\Delta \quad \tilde{z}]^T$ and N_1 is a positive definite diagonal matrix given by

$$N_1 = diag\left[M \quad 1 \quad K^{-1}\right] \qquad (41)$$

In the ideal case $\Delta u_a = 0$ and, according to the expressions (30) and (37), the time derivative of (39) is given by

$$\dot{V} = -(K_D + \sigma_0\sigma_1 K)s^2 - K_P \tilde{p}_\Delta^2 - \frac{m(\dot{y})\sigma_0 K^{-1}}{g(\dot{y})}\tilde{z}^2$$
$$+ \frac{m(\dot{y})\sigma_0\sigma_1}{g(\dot{y})}s\tilde{z} + \frac{\sigma_0\sigma_1\Delta(\dot{y})}{g(\dot{y})}sz - K^{-1}\frac{\sigma_0\Delta(\dot{y})}{g(\dot{y})}z\tilde{z} \qquad (42)$$

Written in a matrix equation form this expression results:

$$\dot{V} = -\rho^T N_2 \rho + \rho^T D(\rho) \qquad (43)$$

where

$$N_2 = \begin{bmatrix} (K_D + \sigma_0\sigma_1 K) & 0 & -\dfrac{1}{2}\dfrac{\sigma_0\sigma_1}{g(\dot{y})}m(\dot{y}) \\ 0 & K_p & 0 \\ -\dfrac{1}{2}\dfrac{\sigma_0\sigma_1}{g(\dot{y})}m(\dot{y}) & 0 & \dfrac{\sigma_0 K^{-1}}{g(\dot{y})}m(\dot{y}) \end{bmatrix} \qquad (44)$$

$$D(\rho) = \left[\frac{\sigma_0 \sigma_1 \Delta(\dot{y})}{g(\dot{y})} z \quad 0 \quad -\frac{\sigma_0 K^{-1} \Delta(\dot{y})}{g(\dot{y})} z \right]^T \quad (45)$$

The matrix N_2 is state dependent. Specifically it depends on the function $g(\dot{y})$ defined in (9) and on the function $m(\dot{y})$, used in order to smooth $|\dot{y}|$ in equation (23). In the sequence we establish the conditions to make this matrix be uniformly positive definite.

To this end, first we observe that the function $m(\dot{y})$ is equal to zero in the static friction range ($\dot{y} = 0$), and positive ($m(\dot{y}) > 0$) if $\dot{y} \neq 0$.

Out of the static friction range, with $\dot{y} \neq 0$, using the Gershgorin theorem it should be observed that the matrix N_2 in (44) is positive definite if:

i) $\left| \frac{\sigma_0 K^{-1}}{g(\dot{y})} m(\dot{y}) \right| > \left| -\frac{1}{2} \frac{\sigma_0 \sigma_1}{g(\dot{y})} m(\dot{y}) \right|$, and

ii) $\left| K_D + \sigma_0 \sigma_1 K \right| > \left| -\frac{1}{2} \frac{\sigma_0 \sigma_1}{g(\dot{y})} m(\dot{y}) \right|$.

From (i) it results that:

$$K < \frac{2}{\sigma_1} \quad (46)$$

Taken into account that the function $m(\dot{y})$ grows as the velocity grows, consider that, given an initial condition, an upper limit to the velocity, $\dot{y}_{max}$, exists. This implies that an upper limit to $m(\dot{y})$ ($m(\dot{y}) \leq \overline{m}$ $t > 0$) also exists.

Since the function $g(\dot{y})$ is bounded by the static friction force F_s, for the given initial condition expression (ii) gives:

$$K_D > \sigma_0 \sigma_1 \left(\frac{1}{2} \frac{\overline{m}}{F_s} - K \right) \quad (47)$$

It should be observed that K_D is a positive constant and so the following additional restriction should be satisfied:

$$K < \frac{1}{2} \frac{\overline{m}}{F_s} \quad (48)$$

Under conditions (46), (47) and (48), the matrix N_2 results uniformly positive definite, i.e.:

$$N_2 \geq \alpha I \quad (49)$$

where α is a positive constant given by:

$$\alpha = \inf_{t \in [0,T]} \lambda_{min}(N_2) \quad \forall T \geq 0 \quad (50)$$

Using (49) in (43) and employing the Rayleight-Ritz theorem, it can be written that

$$\dot{V} \leq -\alpha \|\rho\|^2 + \|\rho\| \|D(\rho)\| \quad (51)$$

Expression (45) allows the observation that the disturbance $D(\rho)$ is caused by the bounded elastic deflection z and by the residual difference $\Delta(\dot{y}) \geq 0$, defined in (24), which is equal to zero

as the velocity $\dot{y}$ is null or as $\dot{y} \to \pi/2k_v$, and is limited otherwise. So we may establish a superior limit for $\|D(\rho)\| \leq \overline{D}$. Therefore:

$$\dot{V} \leq -\alpha \|\rho\|^2 + \overline{D} \|\rho\| \quad (52)$$

The condition in which the time derivative $\dot{V}$ is negative is given by:

$$\|\rho\| > \frac{\overline{D}}{\alpha} \quad (53)$$

By the Rayleight-Ritz theorem the expression (40) results

$$V = \frac{1}{2} \rho^T N_1 \rho < \frac{1}{2} \lambda_{max}(N_1) \|\rho\|^2 \quad (54)$$

Using the condition (53) in (54) allows to verify that the region in which the function V is negative is limited by a constant value. Expressions (52) and (54) show that $\|\rho\|$ tends to a residual set as $t \to \infty$. Expression (53) outlines that this residual set depends on the value of the disturbance bound $\overline{D}$ and on the value α defined in (50). Consequently each error vector component tends to a residual. This means that the velocity error measure $s(t)$ tends to a residual set. This error can be interpreted as an input of the first order filter given in (27), and based on this interpretation we conclude that the tracking errors $\dot{\tilde{y}}(t)$ and $\tilde{y}(t)$ tend to a residual set as $t \to \infty$. This completes the proof.

Remark 1: As $\dot{\tilde{y}}(t)$ tends to a limited residual set, and as the desired velocity $\dot{y}_d(t)$ is also limited, from the error definition in (27) it results that the velocity $\dot{y}(t)$ is limited, i.e., there is an upper bound $\dot{y}_{max}$ as considered above, which depends on the closed loop system dynamics and on the initial conditions.

Remark 2: From remark 1 it is clear that the initial conditions should be chosen in order to satisfy the conditions (47) and (48). Therefore, the theorem result depends on the initial conditions, and so, it is a local result.

Remark 3: The "disturbance" upper bound ($\overline{D}$) depends on the friction characteristics (see (45)) and on the smoothing function $m(\dot{y})$. The positive constant α defined in (50) depends on the controller gains. Therefore, the residual set given by (53) depends on the friction characteristics, on the smoothing function and on the controller gains.

The experimental results presented in the next section validate these theoretical statements.

Experimental Results

The parameters used in the experiments are: $A = 4.19 \times 10^{-4}$ [m^2], $r = 1.4$, $R = 286.9$ [J Kg/K], $T = 293.15$ [K], $L = 1$ [m], $V_{10} = 1.96 \times 10^{-6}$ [m^3], $V_{20} = 4.91 \times 10^{-6}$ [m^3] and $M = 2.9$ [Kg]. All experimental tests were realized without applying external forces ($F_e = 0$).

The mass flow functions $q_{mi}(p_i, u)$ defined in Eq. (4) and (5), are identified according to the methodology presented in Perondi and Guenther (2003). This allows the calculation of the servovalve control voltage using the inverse defined in Eq.(38) (see Perondi and Guenther, 2003, for details).

The experimental tests are performed using a sinusoidal and a polynomial desired trajectory. The sinusoidal desired trajectory is given by $y_d(t) = y_{máx} \sin(wt)$, $y_{máx} = 0,45$ [m] and $w = 2$ [rad/s] (see Fig. 5a).

The polynomial trajectory starts with the piston at 0.05 [m] measured from the end of the cylinder ($y_d(0) = 0,05$ [m]), and reaches a steady-state trajectory at $y_d(2) = 0,95$ [m] according to a function described by the 7th order polynomial given in (55). This position is maintained for 2 [s]. Then, the piston returns to the initial position in 2 [s] according to a polynomial similar to (55), where it stays for 2 [s], and so on. This desired trajectory is shown in figures 5 and can be described by equations (55) and (56).

$$y_{dp}(t) = -6t^7 + 21t^6 - 25,2t^5 + 10,5t^4 \qquad (55)$$

The mechanical subsystem controller is designed according to Eq. (26) using equations (21) and (23). The pneumatic subsystem controller is given by Eq. (31), and by the calculation of the auxiliary signal u_a through Eq. (35), as in the ideal case ($u_a = u_a^*$).

$$
\begin{array}{lll}
& [m] & \\
y_d(t) = & 0.05 + y_{dp}(t/2) & t < 2 \\
& 0.95 & 2 \geq t < 4 \\
& 0.95 - y_{dp}((t-4)/2) & 4 \geq t < 6 \\
& 0.05 & 6 \geq t < 8 \qquad (56)
\end{array}
$$

In order to obtain a response without actuator vibrations and a sufficiently smooth control signal, the control gains are chosen as $K_D = 40$, $\lambda = 20$, $K_P = 150$, and the friction force observer parameters are $\sigma_0 = 4500$, $\sigma_1 = 93.13$, $\sigma_2 = 89.86$, $v_s = 0.02$ [m/s], $F_c = 32.9$ [N], $F_s = 38.5$ [N], $K = 2.22 \times 10^{-6}$.

In the experimental implementation, the velocity is obtained using a filter and a numeric derivative process and the acceleration is calculated based on the nominal parameters.

Figure 4 presents the polynomial desired trajectory, the response to this trajectory using the cascade controller with friction compensation and the tracking error obtained in this case. In order to outline the friction compensation effect, Fig.5 shows the response obtained without this compensation and the respective tracking error. The tracking errors for both cases are presented in detail in Fig. 6. while Fig. 7 shows the control signal using friction compensation.
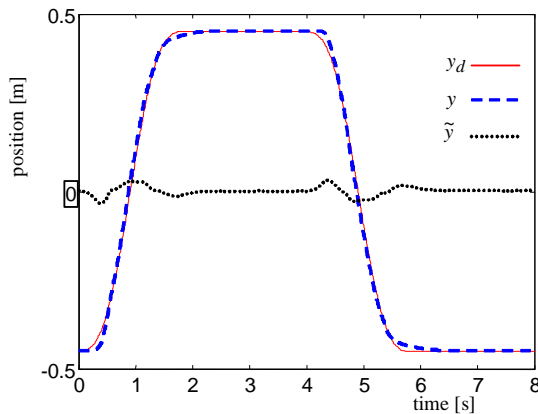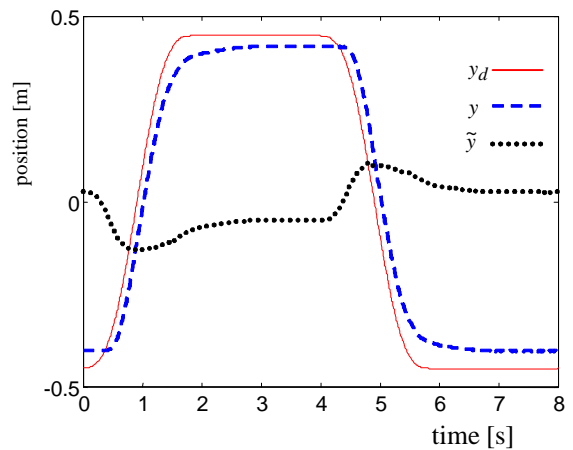
Figure 5. Polynomial y, y_d **and** $\tilde{y}$ **trajectories without friction compensation.**

The results presented in Figures 4, 5, 6 and 7 outline the efficiency of the proposed friction compensation in diminishing the trajectory tracking errors and the steady state position error. These experimental results confirm the tracking error convergence theoretically established.
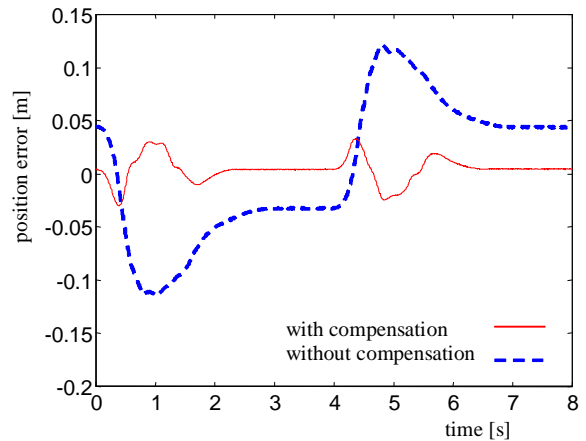
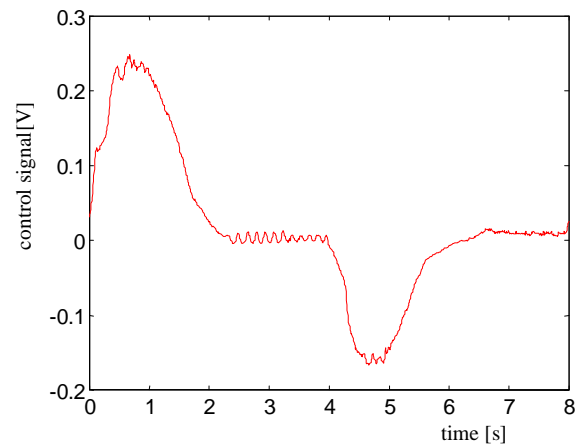**Figure 6. Polynomial tracking position error for both cases.**

Figure 4. Polynomial y, y_d **and** $\tilde{y}$ **trajectories with friction compensation.**

Figure 7. Control signal *u* **(with friction compensation) for the polynomial tracking case.**
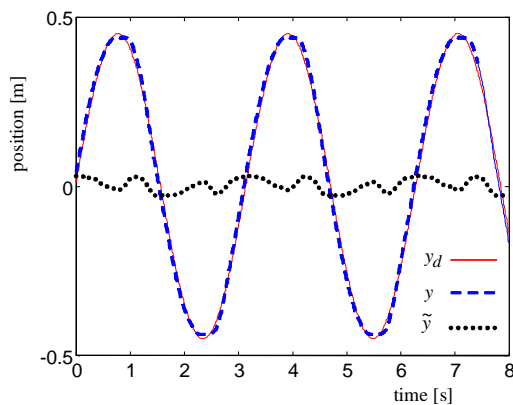
Figure 8. Sinusoidal y, y_d and $\tilde{y}$ trajectories with friction.

Figure 8 presents the desired sinusoidal trajectory, the response to this trajectory using the cascade controller with friction compensation and the tracking error obtained in this case. Figure 9 shows the response obtained without this compensation and the respective tracking error.
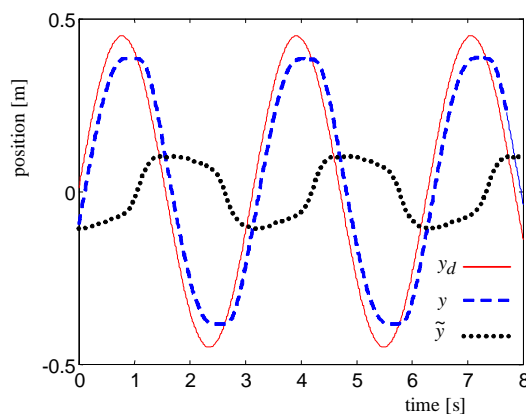

Figure 9. Sinusoidal y, y_d and $\tilde{y}$ trajectories without friction compensation.

The tracking errors for both cases are presented in detail in Fig. 10. Figure 11 shows the control signal using friction compensation. These experimental results confirm the importance of the friction compensation.

Conclusions

In this work a cascade controller with friction compensation for a pneumatic positioning system was proposed, and the convergence of its tracking errors was theoretically and experimentally demonstrated. It was outlined that the cascade control strategy allows the use of the LuGre friction model without any assumptions about the force response in the actuator. The experimental results confirm the theoretical results and demonstrate the efficiency of the friction compensation. Future research will include methods to deal with the system parameter uncertainties.
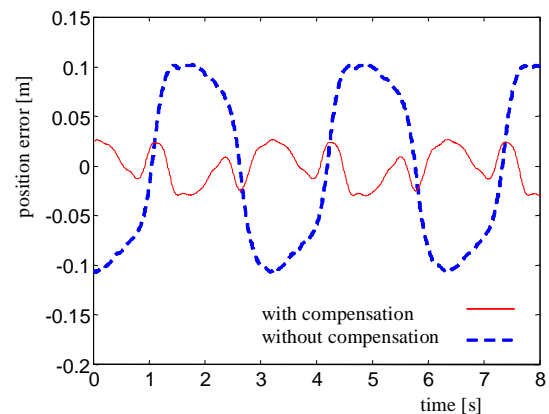

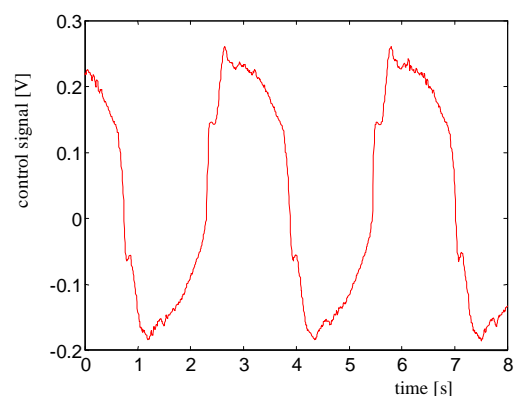**Figure 10. Sinusoidal tracking position error for both cases.**

Figure 11. Control signal u (with friction compensation).

Acknowledgements

References

Armstrong-Hélouvry, B., Dupont P. and Canudas de Wit, C., 1994, "A Survey of Models, Analysis Tools, and Compensation Methods for Control of Machines with Friction", *Automatica*, Vol. 30, n. 7, pp.1083-1138.

Canudas de Wit, C., Olsson, H., Astrom, K.J. and Lischinsky, P., 1995, "A New Model for Control Systems with Friction", *IEEE Transactions on Automatic Control*, Vol. 40, n. 3, pp.419-425.

Guenther, R. and Hsu, L., 1993, "Variable Structure Adaptive Cascade Control of Rigid-Link Electrically Driven Robot Manipulators", *Proc. IEEE 32nd CDC Conference on Decision and Control*, San Antonio, Texas, USA, pp.2137-2142.

Guenther, R. and De Pieri, E.R.,1997, "Cascade Control of the Hydraulic Actuators", *Revista Brasileira de Ciências Mecânicas*, ABCM, Vol. 19, n. 2, pp. 108-120.

Guenther R., Cunha, M.A.B., De Pieri, E.R. and De Negri, V.J, 2000, "VS-ACC Applied to a Hydraulic Actuator", *Proc. of the American Control Conference 2000*, Chicago, USA, pp. 4124-4128.

Guenther R. and Perondi, E.A., 2002 , "O Controle em Cascata de um Sistema Pneumático de Posicionamento", *Anais do XIV Congresso Brasileiro de Automática - CBA 2002*, Natal, RN, pp.936-942.

Hsu, L. and Guenther, R., 1993 , "Variable Structure Adaptive Cascade Control of Multi-Link Robot Manipulators with Flexible Joints: The Case of Arbitrary Uncertain Flexibilities", *Proc. IEEE Conference in Robotic Automation*, Atlanta, Georgia, USA, pp340-345.

Khalil,H. K., 1996, "Nonlinear systems", 2nd edition, New Jersey, USA, Prentice Hall Inc.

Lischinsky, P., Canudas de Wit, C. and Morel, G., 1999 , "Friction Compensation for an Industrial Hydraulic Robot", *IEEE Control Systems*, pp. 25-32, February.

Perondi E. and Guenther, R.,, 2003, "Modeling of a Pneumatic Positioning System", *Science & Engineering Journal,* 01/2003.

Slotine, J-J.E. and Li, W., 1988 , "Adaptive Manipulator Control: A Case Study", *IEEE Transactions on Automatic Control*, Vol. 33, n. 11, pp. 995-1003,.

Utkin, V.I. 1987, "Discontinuous Control Systems: State of Art in Theory and Applications", *IFAC World Congress on Automatic Control. Preprints*, Munich, Germany, Vol.1, pp75-94.